Advances in Difference Equations
a SpringerOpen Journal

RESEARCH Open Access

Fractional-order modelling of state-dependent non-associated behaviour of soil without using state variable and plastic potential

Yifei Sun[1*] and Changjie Zheng[2]

*Correspondence:
sunny@hhu.edu.cn
[1]Key Laboratory of Ministry of Education for Geomechanics and Embankment Engineering, College of Civil and Transportation Engineering, Hohai University, Nanjing, China
Full list of author information is available at the end of the article

Abstract

It was found that the constitutive behaviour of granular soil was dependent on its density and pressure (i.e. material state). To capture such state dependence, a variety of state variables were empirically proposed and introduced into the existing plastic potential functions, which inevitably resulted in the complexity and meaninglessness of some model parameters. The purpose of this study is to theoretically investigate the state-dependent non-associated behaviour of granular soils without using predefined plastic potential and state variable. A novel state-dependent non-associated model for granular soils is mathematically developed by incorporating the stress-fractional operator into the bounding surface plasticity. Unlike previous studies using empirical state variables, the soil state and non-associativity in this study are considered via analytical solution, where a state-dependent plastic flow rule and the corresponding hardening modulus without using additional plastic potentials are obtained. Possible mathematical connection with a well-known empirical state variable is also discussed. The non-associativity between plastic flow and loading directions as well as material hardening is found to be controlled by the fractional-derivative order. To validate the proposed approach, a series of drained and undrained triaxial test results of different granular soils are simulated and compared, where a good agreement between the model predictions and the corresponding test results is observed.

Keywords: Fractional plasticity; Constitutive relations; State dependence; Granular soils

1 Introduction

It has been widely acknowledged that the strength and deformation behaviour of granular soil, such as sand and rockfill, is significantly dependent on its density and pressure (material state) [1]. Before the proper consideration of state dependence during constitutive modelling, different model parameters were often required for modelling the stress-strain behaviour of granular soils with different initial densities or subjected to different confining pressures [2–4].

For the purpose of better understanding and unified constitutive modelling of granular soils, a variety of different empirical state variables have been suggested, such as the state

ratio of the difference between the threshold and current void ratios to the difference between the threshold and critical void ratios [5], the ratio of the current to critical void ratios [6], the disturbance in disturbed state concept [7], the stress ratio of the current to critical mean effective stresses [8] and the most widely used state variable (ψ) defined by the difference between the current and critical state void ratios [9]. It can be found that developing a reasonable state-dependent non-associated plastic flow rule (or stress-dilatancy relationship) has been of the utmost importance in recent years. One of the popular approaches was to modify the existing stress-dilatancy equations, for example, the Cam-clay (CC) stress-dilatancy equation [10] and Rowe's stress-dilatancy equation [11], by empirically incorporating ψ [12–16]. Undeniably, this approach can always substantially improve the model performance; however, the empirical correlation between the state variable and the existing constitutive parameters would inevitably result in more model parameters. It was found that the fractional mechanics was an efficient way to capture the relaxation [17], diffusion [18–20], and stress-strain [14, 21] behaviour of materials. To reduce the number of model parameters without the loss of modelling capability, Sun and Shen [21] proposed a non-associated plastic flow rule for granular soil by simply conducting fractional-order derivatives of the yielding surface, where the obtained vector (plastic flow direction) was no longer normal to the yielding surface, even without using an additional plastic potential. This non-normality increased as the fractional order (α) decreased [14, 22, 23]. To consider the state dependence, the state-dependent fractional plasticity model was then proposed [14] by empirically incorporating ψ, which however made the parameters of the obtained stress-dilatancy equation lack physical meaning.

This study attempts to theoretically investigate the state-dependent non-associated stress-strain behaviour of granular soils. A state-dependent non-associated constitutive model without using any empirical state variables and plastic potentials is developed by using strict mathematics. Instead of modelling the dependence of soil state by empirically incorporating state variables, analytical derivations of the state-dependent plastic flow rule and the associated hardening rule are presented. As the fractional derivative is defined in integral form, the soil state is captured through the integrating range from the lower limit (current stress state) to the upper limit (critical stress state). This paper is divided into four main parts: Sect. 2 defines the basic constitutive relations and the relevant fractional derivative used in this study; Sect. 3 develops a novel state-dependent constitutive model without using plastic potential, where the state-dependent fractional plastic flow rule is analytically derived; Sect. 4 presents the identification and sensitivity analysis of model parameters; Sect. 5 provides the model validation against a series of laboratory test results of different granular soils; Sect. 6 concludes the study. For the sake of simplicity, all the derivations and discussions in this study are limited to homogenous and isotropic materials.

2 Notations and definitions

2.1 Constitutive relations

Following the conventional assumption in soil mechanics, compressive stress and strain are considered as positive while the extensive ones are negative. All the stress mentioned in this study is effective stress obtained by using Terzhgi's effective stress principle. In the elastoplastic model, there are four main parts, i.e. the elastic stiffness tensor (**E**), plastic loading tensor (**m**), plastic flow tensor (**n**) and hardening modulus (H). Accordingly, the

total strain (ε_{ij}) can be decomposed into the following elastic (ε_{ij}^{e}) and plastic (ε_{ij}^{p}) parts:

$$\Delta\varepsilon_{ij} = \Delta\varepsilon_{ij}^{e} + \Delta\varepsilon_{ij}^{p}, \tag{1}$$

where $i, j = 1, 2, 3$. Δ indicates increment, while the superscripts e and p imply the elastic and plastic components, respectively. Based on Hooke's law, the incremental elastic strain tensor ($\Delta\varepsilon_{ij}^{e}$) can be correlated to the incremental effective stress tensor ($\Delta\sigma_{ij}'$) by

$$\Delta\sigma_{ij}' = E_{ijkl}\Delta\varepsilon_{kl}^{e}, \tag{2}$$

where E_{ijkl} denotes the fourth-order elastic stiffness tensor, which can be defined as follows [24]:

$$E_{ijkl} = (K - 2G/3)\delta_{ij}\delta_{kl} + G(\delta_{ik}\delta_{jl} + \delta_{il}\delta_{jk}), \tag{3}$$

in which δ_{ij} is the Kronecker delta. K and G are the bulk and shear moduli, respectively, which can be expressed by using [25]

$$K = \frac{1+e}{\kappa}p', \tag{4}$$

$$G = \frac{3(1-2\nu)}{2+2\nu}K, \tag{5}$$

where κ is the gradient of the swelling line in the $e - \ln p'$ plane; e is the current void ratio of the sample; ν is Poisson's ratio. $p' = \sigma_{ij}'\delta_{ij}/3$ is the mean effective principal stress. In addition, the generalised shear stress $q = \sqrt{3/2 s_{ij}s_{ij}}$, in which $s_{ij} = \sigma_{ij}' - \sigma_{kk}'\delta_{ij}/3$, is the deviatoric stress tensor. The corresponding volumetric strain (ε_v) can be defined as $\varepsilon_v = \varepsilon_{ij}\delta_{ij}$, while the generalised shear strain $\varepsilon_s = \sqrt{2/3 e_{ij}e_{ij}}$, where $e_{ij} = \varepsilon_{ij} - \varepsilon_v\delta_{ij}$, is the deviatoric strain tensor.

In plasticity approach, the incremental plastic strain tensor ($\Delta\varepsilon_{ij}^{p}$) can be related to incremental effective stress tensor such that [26]

$$\Delta\varepsilon_{ij}^{p} = \frac{1}{H}n_{ij}m_{kl}\Delta\sigma_{kl}', \tag{6}$$

where the plastic loading tensor (m_{ij}) is normal to the yielding surface and thus can be determined by conducting first-order derivative of the yielding surface; the plastic flow tensor (n_{ij}) is non-normal to the yielding surface for non-associative geomaterials and can be determined by conducting fractional-order derivative of the yielding surface, as shown in Sumelka and Nowak [23] and Sun et al. [27]; the hardening modulus (H) for granular soils involves both the size hardening and a relative position of the yielding surface with respect to the bounding surface, and it will be defined later. Combining Eqs. (2)–(6), the following elastoplastic constitutive relation can be given:

$$\Delta\sigma_{ij}' = \left[E_{ijkl} - \frac{E_{ijct}n_{ct}E_{klrs}m_{rs}}{H + m_{ct}E_{ctab}n_{ab}}\right]\Delta\varepsilon_{kl}. \tag{7}$$

2.2 Fractional derivative and yielding surface

There are many different definitions of fractional derivatives [17–20, 28, 29], where each of them is in integral form and somehow complex. Therefore, only some of the functions, for example, the power-law function, have certain analytical solution, whereas the rest need numerical approximation [30, 31]. Following the fractional plasticity [14, 22, 32], the following well-known Caputo's left-sided (Eq. (8)) and right-sided (Eq. (9)) fractional derivatives [33, 34] are used in this study:

$$ {}_{\sigma_c'}D^{\alpha}_{\sigma'}f\left(\sigma'\right) = \frac{1}{\Gamma(n-\alpha)}\int_{\sigma_c'}^{\sigma'}\frac{f^{(n)}(\chi)\,d\chi}{(\sigma'-\chi)^{\alpha+1-n}}, \quad \sigma' > \sigma_c', \tag{8} $$

$$ {}_{\sigma'}D^{\alpha}_{\sigma_c'}f\left(\sigma'\right) = \frac{(-1)^n}{\Gamma(n-\alpha)}\int_{\sigma'}^{\sigma_c'}\frac{f^{(n)}(\chi)\,d\chi}{(\chi-\sigma')^{\alpha+1-n}}, \quad \sigma_c' > \sigma', \tag{9} $$

where D $(= \partial^{\alpha}/\partial\sigma'^{\alpha})$ denotes partial derivation to obtain the fractional stress gradient on the yielding function f. It is noted that Caputo's fractional derivative has singular kernel, which may not be applicable in a more specific case, e.g. capturing material heterogeneities and structures with different scales. A possible solution of this limit is to propose a new fractional derivative without singular kernel, for example, the Caputo–Fabrizio derivative [35] and Yang–Srivastava–Machado derivative [28]. It is worthwhile pointing out that the Yang–Srivastava–Machado fractional derivative [28] is a well-known extension of the Riemann–Liouville fractional derivative with singular kernel, which has great potential in solving local thermal and mechanical problems. However, in this study, only mechanical phenomena related to plasticity are considered; therefore, the original Caputo's fractional derivative [33, 34] is sufficient and effective [35]. Following Sun et al. [27, 36], the modified Cam-clay (MCC) yielding function is used

$$ f = \left(2p' - p_0'\right)^2 + \left(\frac{2q}{M}\right)^2 - p_0'^2 = 0, \tag{10} $$

where the critical state stress ratio M can be expressed as [37]

$$ M = M_c\left[\frac{2c^4}{1 + c^4 - (1-c^4)\sin(3\theta)}\right]^{1/4} \tag{11} $$

in which M_c denotes the critical state stress ratio for triaxial compression; c denotes the ratio between the critical state stress ratio for triaxial extension (M_e) and M_c. The Lode angle (θ) is expressed as $\theta = \arccos\{9s_{ij}s_{jk}s_{ki}/[2(3s_{lr}s_{lr}/2)^{3/2}]\}/3$. $\theta \in [-\pi/6, \pi/6]$, where $\theta = \pi/6$ corresponds to triaxial compression, whereas $\theta = -\pi/6$ corresponds to triaxial extension. p_0' controls the size (hardening) of the yielding surface. Furthermore, in Eq. (9), the gamma function is defined as follows: $\Gamma(x) = \int_0^{\infty} e^{-\tau}\tau^{x-1}\,d\tau$. α is the fractional order and should be at least less than two due to the thermodynamic restriction for a positive plastic dissipation [27]. As discussed in Sun and Shen [21], α represents the extent of non-associativity between plastic flow and loading directions as well as the degree of state dependence of material deformation. σ' is the current effective stress, while σ_c' is the corresponding critical-state stress. The use of σ_c' for integral limit is attributed to the basic assumption

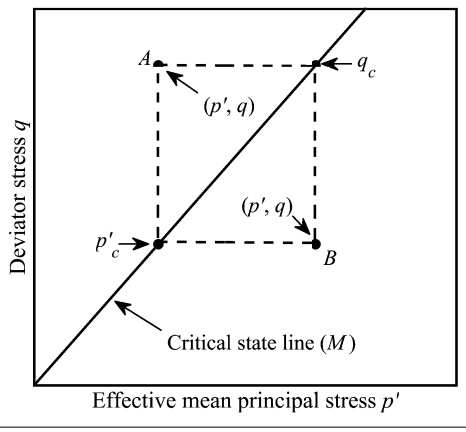

Figure 1 Schematic show of the possible location of current stress point

from the critical state soil mechanics [10]: upon shearing, soil would deform continuously and finally approach the critical state represented by the critical state lines (CSLs) in the $e - \ln p'$ and $p' - q$ planes, respectively, as follows:

$$p'_c = p_r \exp\left(\frac{e_\Gamma - e}{\lambda}\right), \tag{12}$$

$$q_c = q + M\left(p' - p'_c\right), \tag{13}$$

where p_r is the unit pressure; λ is the gradient of the CSL in the $e - \ln p'$ plane. e_Γ denotes the intercept of the CSL at $p' = 1$ kPa. p' and p'_c are the mean effective principal stresses at the current and the corresponding critical states, respectively, while q and q_c are the deviator stresses at the current and corresponding critical states, respectively. It should be noted that in this study we connect the current stress point (p', q) with the corresponding CSL by using the critical state stress ratio M as shown in Fig. 1. Before soil reaches the critical state, there are three possible locations of the current stress point in relation to the CSL in the $p' - q$ plane, i.e. on the "dry" side (above), on the "wet" side (below) and on the CSL. If the current state is on the CSL, then $p' = p'_c$ and $q = q_c$, where only one critical-state stress point is indicated, and the material is currently undergoing critical state flow. However, in the rest two cases, it is observed that p'_c and q_c should represent two independent critical-state stress points (A and B) on the CSL. As shown in Fig. 1, stress point A implies a soil with dilation trend, while stress point B represents a soil with contraction trend. p'_c is obtained by extending a horizontal parallel line from the current stress points (A or B) with regard to the p'-axis and intersecting the CSL, while q_c is obtained by intersecting a vertical parallel line extended from the current stress points (A or B) with regard to the q-axis. The relative location of the current stress point to the critical state line defines which equation, (8) or (9), will be used. More specifically, if $p' > p'_c$ or $q > q_c$, Eq. (8) should be used and vice versa. However, as demonstrated in [36], even if different positions (or definitions) of the current stress point (or fractional derivatives) were used, a unique state-dependent plastic flow rule was obtained without using any plastic potential and empirical state parameters in the end.

3 State-dependent fractional model

3.1 State-dependent plastic flow

In this study, the state-dependent fractional plastic flow tensor (n_{ij}) is defined as

$$n_{ij} = \frac{1}{\sqrt{1+d_g^2}}\left[\frac{d_g}{3}\delta_{ij} + \frac{3s_{ij}}{2q}\right], \tag{14}$$

where d_g is the stress-dilatancy ratio, which has several different definitions by different researchers, for example, the CC expression [26, 38], elliptic expression [12, 39], Rowe's expression [6, 40], etc. However, no matter which kind of dilatancy equation was used in the classical plasticity model, an empirical state index was necessarily incorporated for the unified modelling of state-dependent behaviour of geomaterials subjected to a wide range of densities and pressures [3]. In this study, a three-dimensional state-dependent dilatancy ratio without using empirical state index and plastic potential can be derived by following Sun et al. [27, 36], where the unified stress-dilatancy ratio (d_g) can be obtained by using Eqs. (8) and (9) to perform fractional-order derivatives on the MCC surface such that

$$\begin{aligned} d_g &= -\frac{{}_{p'}D^{\alpha}_{p'_c} f(p')}{{}_{q_c}D^{\alpha}_{q} f(q)} = -\frac{{}_{p'_c}D^{\alpha}_{p'} f(p')}{{}_{q}D^{\alpha}_{q_c} f(q)} \\ &= M^{1+\alpha}\frac{(p'-p'_c)+(2-\alpha)(p'_c-p'_0/2)}{(q-q_c)+(2-\alpha)q_c}, \end{aligned} \tag{15}$$

where the material flow is found to be influenced by several factors, including the Lode angle (θ) via M, current stress (p', q) and critical-state stress (p'_c, q_c); most importantly, it is also determined by the stress distances from the current state to the corresponding critical state ($p'-p'_c$ and $q-q_c$). It is easy to find that $d_g = 0$ at critical state where $p' = p'_c$ and $q = q_c$, indicating no plastic volumetric strain. The fractional gradient on MCC, by using Eqs. (8) and (9), intrinsically considers the state information of soil during shearing. Therefore, unlike classical isotropic and anisotropic plasticity models [41–45] where the influence of material state on plastic flow requires the empirical incorporation of a state parameter (e.g. ψ), a state-dependent plastic flow is mathematically developed in this study. By using Eq. (15), the effect of α on the stress-dilatancy behaviour of granular soil during shearing can be obtained. As shown in Sun et al. [36],the stress-dilatancy curve exhibited clockwise rotation coupled with a downward shifting as α increased. It reduces to the classical MCC stress-dilatancy model [10] with $\alpha = 1$.

It should be also noted that there are only two chances for the stress-dilatancy ratio $d_g = 0$. One is at the critical state and the other is at the phase transformation state. At critical state where $p' = p'_c$ and $q = q_c$, the stress-dilatancy ratio is automatically equal to zero, indicating no plastic volumetric strain. At the phase transformation state, $d_g = 0$ can be ensured by a proper value of α, which can be defined by rearranging Eq. (16) as follows:

$$\alpha = \frac{2M^2 p'_{ct} - 2\eta_t^2 p'_t}{2M^2 p'_{ct} - M^2 p'_t - \eta_t^2 p'_t}, \tag{16}$$

in which $p'_{ct} = p_r \exp((e_\Gamma - e_t)/\lambda)$; e_t, p'_t and η_t are the void ratio, effective mean principal stress and stress ratio, respectively, at the phase transformation state. Due to the use of the vertical ($q-q_c$) and horizontal ($p'-p'_c$) distances through α, the phase transformation line

is not fixed but changed with the initial material state. For further clarification, an analogy of the function of α with that of the state parameter (m) in Li and Dafalias [1] can be made, where m was used to capture the state-dependent plastic flow and ensured the variation of the phase transformation line with material state. Therefore, a state-dependent plastic flow is analytically developed.

3.2 Possible mathematical connection with I_p

Another interesting finding on the mathematical connection with the empirical state variable I_p [8] can be made by further substituting Eq. (13) into Eq. (15). Then, the above stress-dilatancy equation can be rearranged as follows:

$$\begin{aligned} d_g &= M^{1+\alpha}\frac{(I_p-1)+(2-\alpha)[1-I_p/2-I_p\eta^2/(2M^2)]}{(1-I_p)M+(2-\alpha)[q/p'_c+M(I_p-1)]} \\ &= M^{\alpha}\frac{[\alpha/2-(1-\alpha/2)\eta^2/M^2]I_p+(1-\alpha)}{(1-I_p)+(2-\alpha)[q/Mp'_c+(I_p-1)]}, \end{aligned} \tag{17}$$

where $I_p = p'/p_c$ is the state pressure index defined by Wang et al. [8]. A mathematical connection between the derived stress-dilatancy ratio and the empirical state pressure index I_p is observed. Unlike other studies [46] that empirically incorporated I_p, the current study reflects the dependence of state pressure from the natural mathematical derivation. However, it should be noted that the relation between d_g and I_p in particular ties this model to other models [1, 13–15, 41, 47] that used I_p or ψ [9] with the added advantage of deriving such relation by conducting fractional derivative of a specific (e.g. MCC) yield surface. Does this connection also generally exist when using other yielding surfaces? Further studies need to be carried out. Nevertheless, it should be emphasized that due to the integral definition of the fractional derivative, the fractional approach proposed in this study intrinsically considers the state information from current state to critical state, as indicated in the initial definition of the fractional derivatives shown in Eqs. (8) and (9). One can also theoretically derive a state-dependent stress-dilatancy equation by conducting fractional derivative of other yielding surfaces.

3.3 Bounding surface and loading direction

For the sake of simplicity, the bounding surface ($\bar{f}$) is assumed to have the same shape as the yielding surface, i.e.

$$\bar{f} = \left(2\bar{p}' - \bar{p}'_0\right)^2 + \left(\frac{2\bar{q}}{M}\right)^2 - \bar{p}'^2_0 = 0, \tag{18}$$

where $\bar{p}'_0$ is the intercept of the bounding surface with the abscissa, controlling the size of the bounding surface. The image stress point $(\bar{p}', \bar{q})$ on the bounding surface can be expressed by employing a scalar ρ as

$$\bar{p}' = \rho\bar{p}'_0 \tag{19}$$

$$\bar{q} = \rho\eta\bar{p}'_0, \tag{20}$$

in which the stress ratio η can be defined by using the radial mapping rule [39] as follows:

$$\eta = \frac{q}{p'} = \frac{\bar{q}}{\bar{p}'}. \tag{21}$$

In bounding surface plasticity [48], the loading tensor (m_{ij}) is normal to the bounding surface and therefore can be obtained by conducting first-order derivative of the bounding surface function as follows:

$$m_{ij} = \frac{1}{\sqrt{1 + d_f^2}} \left[\frac{d_f}{3} \delta_{ij} + \frac{3 s_{ij}}{2q} \right], \tag{22}$$

where the loading ratio d_f is formulated as

$$d_f = \frac{M^2 - \eta^2}{2\eta}. \tag{23}$$

Further substituting Eqs. (19)–(21) into Eq. (18), the scalar (ρ) which determines the image stress point can be obtained as follows:

$$\rho = \frac{1}{1 + (\eta/M)^2}. \tag{24}$$

In addition, the position of the initial bounding surface ($\bar{p}'_{0i}$) can be further obtained by intersecting the normal compression and swelling lines in the $e - p'$ plane as follows:

$$\bar{p}'_{0i} = 2 p_r \exp\left[\frac{e_\Gamma - e_0 - \kappa \ln p'_{ic}}{\lambda - \kappa} \right], \tag{25}$$

where e_0 is the initial void ratio prior to shearing. p'_{ic} is the initial confining pressure. The evolution of the bounding surface ($\bar{p}'_0$) can be further obtained as follows:

$$\bar{p}'_0 = \bar{p}'_{0i} \exp\left(\frac{1 + e_0}{\lambda - \kappa} \varepsilon_v^p \right). \tag{26}$$

Note that detailed derivations of Eqs. (25) and (26) can be found in Sun and Shen [21] and Sun et al. [49], thus not repeated here for simplicity.

3.4 Hardening modulus

According to Dafalias [48], the hardening modulus H is determined by both the size (hardening) of the bounding surface and the distance between the loading and bounding surfaces. H was also observed to depend on the material state where a state variable was usually empirically incorporated, for example, in Wang et al. [8]. It is usually decomposed into two components [12, 39, 47]:

$$H = H_b + H_\delta, \tag{27}$$

where H_b is determined by applying consistency condition on the bounding surface that experiences isotropic hardening:

$$H_b = -\frac{\partial \bar{f}}{\partial \bar{p}'_0}\frac{\partial \bar{p}'_0}{\partial \varepsilon_v^p}\frac{n_v}{\|\frac{\partial \bar{f}}{\partial \bar{\sigma}}\|} = \frac{1+e_0}{\lambda-\kappa}\frac{\bar{p}' M_c^2 d_g/\sqrt{d_g^2+1}}{\sqrt{(2\rho-1)^2 M_c^4 + 4\rho^2\eta^2}}. \tag{28}$$

It is easy to find that H_b is state-dependent due to the dependence of d_g on material state. H_δ is related to the ratio between the distance (δ) from the current stress point to the image stress point and the distance ($\delta_{\max}$) from the stress origin to the image stress point [21, 39]:

$$H_\delta = h_0 p' \frac{1+e_0}{\lambda-\kappa}\frac{\delta}{\delta_{\max}-\delta}, \tag{29}$$

where $h_0 = h_1 e - h_2$; h_1 and h_2 are material constants. As expected, the hardening modulus $H = +\infty$ at the load onset where $\delta_{\max} - \delta \to 0$, $\eta = 0$ and $\dot{\eta} = 0$, indicating a state of no plastic strain. $H = 0$ at the critical state where $p' = p'_c$, $q = q_c$, $\bar{p}'_0 = p'_0$.

4 Parameter identification and sensitivity analysis

There are totally nine parameters (M_c, λ, e_Γ, c, α, h_1, h_2, κ, ν) in the proposed state-dependent model, which can be all determined from traditional triaxial tests. Detailed elaborations on parameter identification and sensitivity analysis are given below.

Similar to the classical plasticity models, there are four critical state parameters, i.e. M_c, λ, e_Γ and c. The critical state stress ratio (M_c) is determined by measuring the gradient of the critical state line in the $p' - q$ plane. With the increase of M_c, the predicted shear strength of granular soil increases while the volumetric dilation decreases, as shown in Fig. 2. Note that the other model parameters used for simulations in Fig. 2 are: $\lambda = 0.057$, $e_\Gamma = 0.64$, $c = 1$, $\alpha = 1.12$, $h_1 = h_2 = 2.5$, $\kappa = 0.0013$ and $\nu = 0.25$.

λ and e_Γ are the critical state parameters in the $e - \ln p'$ plane. λ can be obtained by measuring the gradient of the critical state line in the $e - \ln p'$ plane, while e_Γ can be determined by the intercept of the critical state line at $p' = 1$. c can be determined by further conducting a triaxial extension test to obtain the critical state stress ratio (M_e) for triaxial

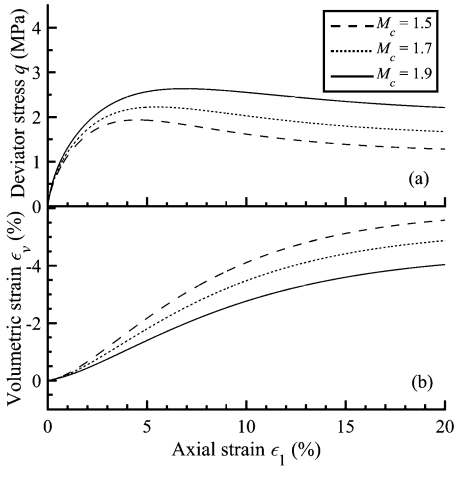

Figure 2 Effect of M_c on the stress-strain behaviour of granular soil

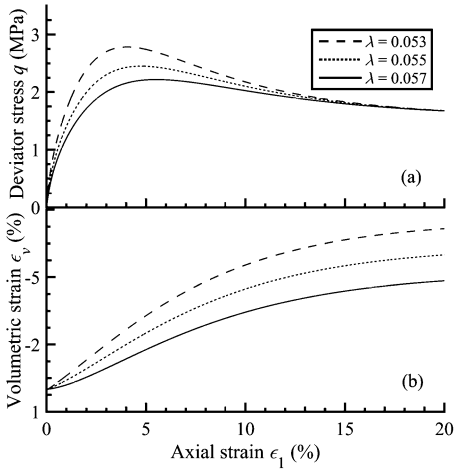

Figure 3 Effect of λ on the stress-strain behaviour of granular soil

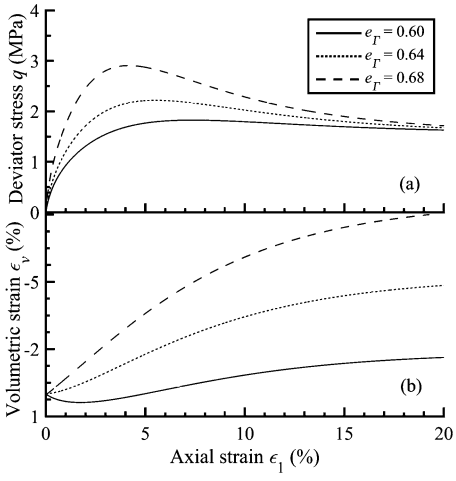

Figure 4 Effect of e_Γ on the stress-strain behaviour of granular soil

extension and then $c = M_e/M_c$. As shown in Fig. 3, with the increase of λ, the predicted peak stress and volumetric dilation decrease. However, as shown in Fig. 4, with the increase of e_Γ, the predicted peak stress and volumetric dilation increase. Note that the other model parameters used for simulations in Figs. 3 and 4 are: $M_c = 1.7$, $c = 1$, $\alpha = 1.12$, $h_1 = h_2 = 2.5$, $\kappa = 0.0013$ and $\nu = 0.25$.

There is one new parameter, the fractional order α, that is distinct from the ones in the traditional plasticity model. It controls the state-dependent plastic flow of granular soil. Thus, it can be obtained by using the stress-dilatancy ratio at the phase transformation state, i.e. Equation (16). As shown in Fig. 5, with the increase of α, the predicted peak stress decreases while the volumetric dilation increases. Samples modelled by a higher α reach critical state more quickly; a transition from the strain softening behaviour to strain hardening behaviour is also observed when α increases from 1.0 to 1.4. Note that the other model parameters used for simulations in Fig. 5 are: $M_c = 1.7$, $c = 1$, $\lambda = 0.057$, $e_\Gamma = 0.64$, $h_1 = h_2 = 2.5$, $\kappa = 0.0013$ and $\nu = 0.25$.

The hardening parameter h_0 is correlated with the void ratio through h_1 and h_2. As illustrated in Li and Dafalias [1] as well as Sun and Shen [21], they can be obtained by fitting the $\varepsilon_1 - q$ relationship of samples with different void ratios. The effect of h_0 on

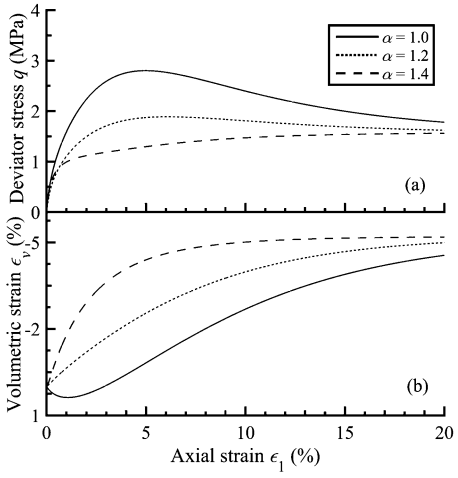

Figure 5 Effect of α on the stress-strain behaviour of granular soil

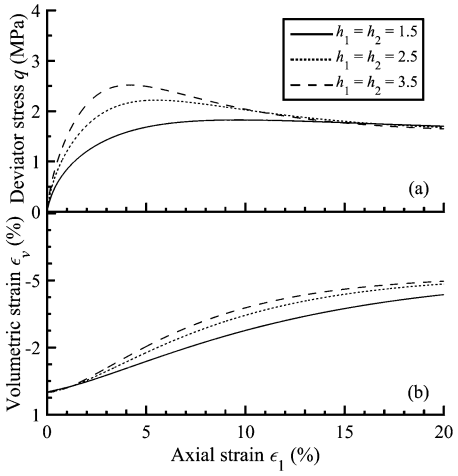

Figure 6 Effects of h_1 and h_2 on the stress-strain behaviour of granular soil

the stress-strain behaviour of granular soil can be found in Fig. 6, where an increasing shear strength coupled with an increasing volumetric dilation is found. Note that the other model parameters used for simulations in Fig. 6 are: $M_c = 1.7$, $c = 1$, $\lambda = 0.057$, $e_\Gamma = 0.64$, $\alpha = 1.12$, $\kappa = 0.0013$ and $\nu = 0.25$.

The elastic constant κ can be determined by measuring the gradient of the swelling line in the $e - \ln p'$ plane. As observed in Fig. 7, with the increase of κ, the peak deviator stress increases, while the initial deviator stress increases more rapidly with a lower κ. In addition, a distinct difference is observed in the relationship between ε_v and ε_1. At the initial loading stage where ε_1 is small, a large volumetric contraction is observed for soils with high κ. However, the effect of κ on ε_v gradually becomes insignificant when ε_1 increases, where the plastic parts of ε_1 and ε_v become dominant.

Poisson's ratio ν defines the lateral deformation ability of the material and can be obtained by using the following equation during the initial loading stage [12]:

$$\nu \approx -\frac{\varepsilon_3}{\varepsilon_1}. \tag{30}$$

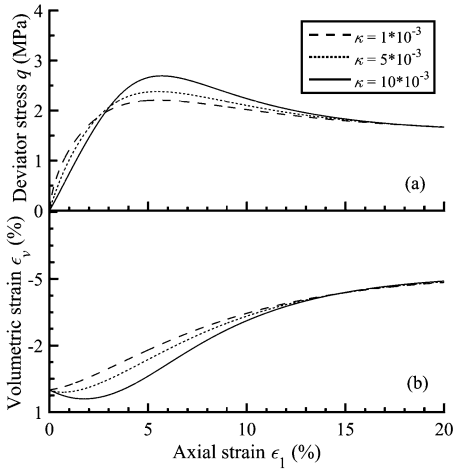

Figure 7 Effect of κ on the stress-strain behaviour of granular soil

Table 1 Model parameters

Soil type	κ (10^{-3})	ν	M_c	λ	e_Γ	α	h_1	h_2
Ottawa sand [50]	5.0	0.25	1.19	0.017	0.864	0.75	0.95	0.35
Sacramento River sand [51]	5.0	0.25	1.40	0.031	1.054	1.10	15	12.7
Tacheng rockfill [12]	1.28	0.25	1.64	0.0568	$0.53 + 0.59e_0$	1.05	15	1.0

The effect of ν was found to be limited and thus not presented here for simplicity. However, according to the theory of elasticity, a higher lateral deformation could be observed with increasing ν. Detailed values of each model parameter used for predicting the stress-strain behaviour of different granular soils are listed in Table 1. It is noted that for simulating triaxial tests with $\theta = \pi/6$, c will not be used.

5 Model validation

This section demonstrates the model's ability to capture the state-dependent constitutive behaviour of different granular soils, including rockfill and sand with different initial states. A series of triaxial tests results of Tacheng rockfill [12], Sacramento River sand [51] and Ottawa sand [50] are simulated in Figs. 8–14. Drained stress-strain behaviour of Tacheng rockfill [12] with four different initial void ratios is simulated in Figs. 8–11, while Figs. 12–14 present the model predictions of the drained and undrained triaxial behaviour of Sacramento River sand [51] and Ottawa sand [50]. It is noted that the all the test results are represented by discrete data points, while continuous lines are used for model predictions.

Xiao et al. [12] reported a series of drained triaxial test results of Tacheng rockfill with different initial void ratios. The material mainly consisted of sub-angular to rounded particles with a median diameter (d_{50}) of 23 mm and a coefficient of uniformity (C_u) of 5.4. Samples were prepared by layered compaction to have a diameter around 300 mm and a height around 600 mm. Initial void ratios and the corresponding confining pressures can be found in Figs. 8–11 and thus not repeated here. It is observed from Figs. 8–11 that even without using the state variable and plastic potential function, the proposed model can well simulate with state-dependent constitutive behaviour of Tacheng rockfill subjected to different initial states (confining pressures and void ratios). The strain hardening

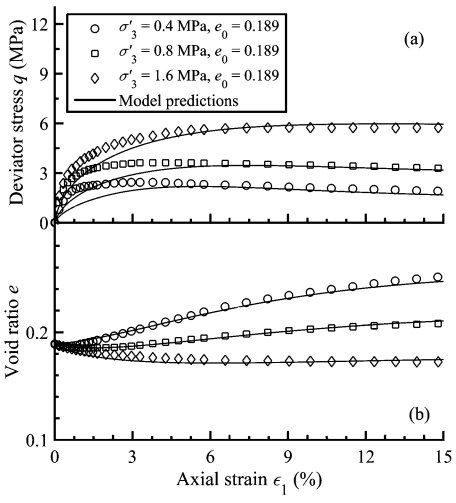

Figure 8 Model predictions of the drained behaviour of Tacheng rockfill with $e_0 = 0.189$ (data from Xiao et al. [12])

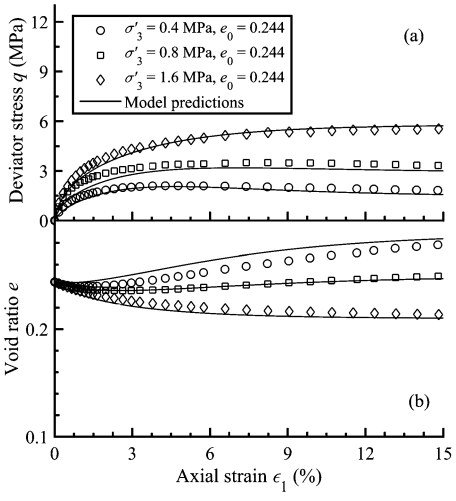

Figure 9 Model predictions of the drained behaviour of Tacheng rockfill with $e_0 = 0.244$ (data from Xiao et al. [12])

and softening behaviour as well as the corresponding volumetric contraction and dilation behaviour of Tacheng rockfill can be all reasonably captured.

Lee and Seed [51] conducted a comprehensive study on the drained and undrained triaxial behaviour of Sacramento River sand under different initial conditions. The Sacramento River sand mainly consisted of sub-round quartz aggregates and occasional shell fragments with a d_{50} of 0.22 mm and a C_u equal to 1.45. The minimum and maximum void ratios were tested to be 0.61 and 1.03, respectively. Samples were prepared to have an initial diameter around 42.67 mm and a height around 103.63 mm. The initial void ratio of 0.87 is used for simulating the drained test results, whereas the initial void ratios of 0.86, 0.86, 0.86 and 0.85 are used for simulating undrained tests carried out under the confining pressures of 98, 294, 490 and 1069 kPa, respectively. Figure 12 shows the model simulations of the drained constitutive behaviour of Sacramento River sand, where a good agreement between the model simulations and the corresponding test results can be observed. Figure 13 shows the model simulations of the undrained behaviour of Sacramento River sand subjected to different initial conditions. As the axial strain increases,

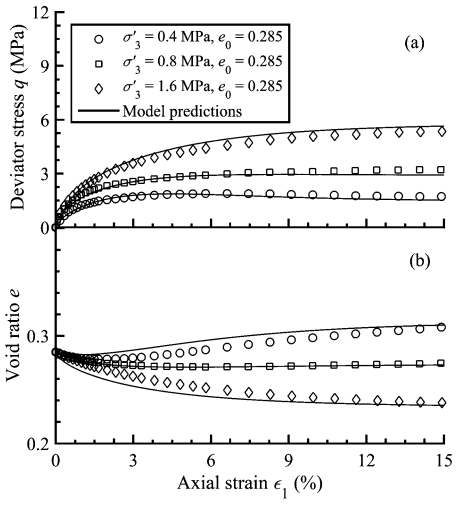

Figure 10 Model predictions of the drained behaviour of Tacheng rockfill with $e_0 = 0.285$ (data from Xiao et al. [12])

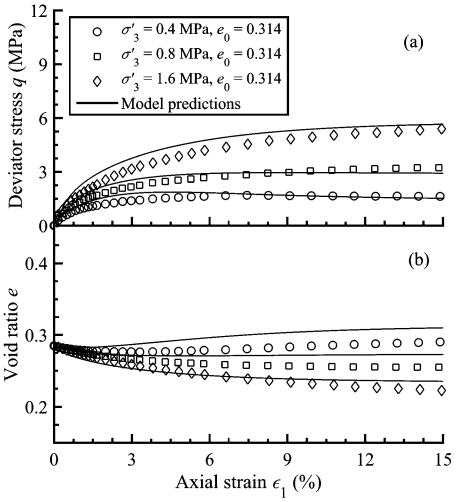

Figure 11 Model predictions of the drained behaviour of Tacheng rockfill with $e_0 = 0.317$ (data from Xiao et al. [12])

the simulated deviator stresses increase until reaching critical (steady) state flow, which is in good agreement with the corresponding test results, which further validates the newly developed state-dependent stress-dilatancy relationship.

Figure 14 presents the simulation results of undrained constitutive behaviour of uniform Ottawa sand [50] that mainly consisted of round/sub-round quartz aggregates. Test results of Ottawa sand with the initial void ratios of 0.793, 0.793 and 0.805 under the respective corresponding confining pressures of 348, 475 and 550 kPa are simulated. It is found that the model predictions match well with the test results. The simulated deviator stress increases initially until reaching a peak value and then decreases significantly at the critical state, indicating a state of static liquefaction of the material. Samples with the same initial void ratios approach the same deviator stress with further shearing, which can be all reasonably characterised by the proposed fractional plasticity model.

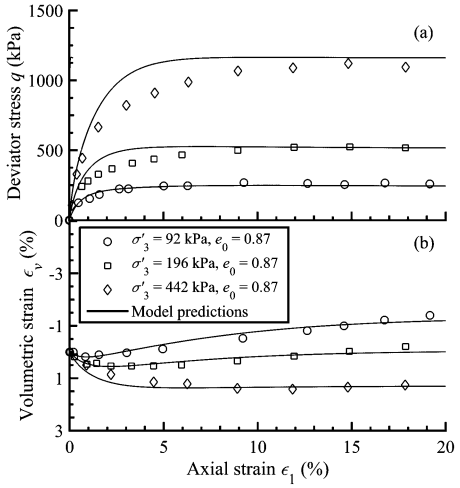

Figure 12 Model predictions of the drained behaviour of Sacramento River sand [51]

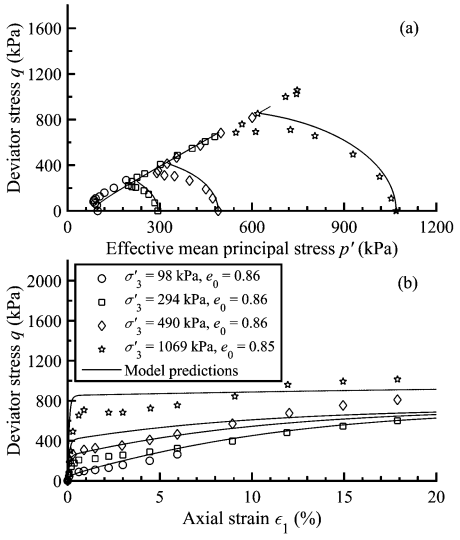

Figure 13 Model predictions of the undrained behaviour of Sacramento River sand [51]

6 Conclusions

It was found that the stress-strain behaviour of granular soil was state-dependent. To capture such state dependence, many sophisticated constitutive models have been proposed by incorporating empirical state variables into additional plastic potential functions. To simplify the modelling approach, a novel state-dependent fractional plasticity model without using predefined state variable and plastic potential was proposed by conducting fractional-order derivatives of the yielding function. Detailed identifications and sensitivity analysis of model parameters were then carried out. To further validate the developed model, a series of drained and undrained test results of different granular soils were simulated and discussed. The main findings are summarized as follows:

(1) Without using predefined state variables and plastic potential functions, a novel state-dependent stress-dilatancy equation was analytically derived by using the fractional-order plasticity theory. Dependence of the non-associated flow on material state was modelled through rigorous mathematical definition of the fractional stress gradient.

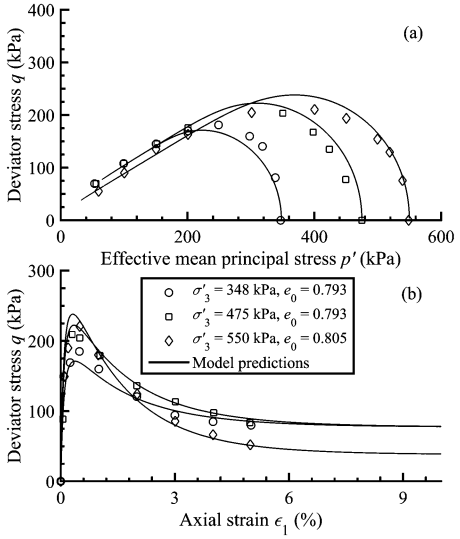

Figure 14 Model predictions of the undrained behaviour of Ottawa sand [50]

(2) Possible mathematical connections between the proposed state-dependent dilatancy equation and the state pressure index by Wang et al. [8] were also discussed, where the dependence of state pressure on the stress-dilatancy phenomenon of granular soil was analytically proved.

(3) The extent of non-associativity and hardening modulus were influenced by the material state via the vertical and horizontal distances from the current stress state to the corresponding critical stress state in the $p' - q$ plane.

(4) With the increase of the fractional order, the predicted peak stress decreased while the volumetric dilation increased. Samples modelled by a higher fractional order reached critical state more quickly; the transition from the strain softening behaviour to strain hardening behaviour also increased with the increase of the fractional order.

(5) Model parameters can be all determined from traditional triaxial test results. It was found that the proposed state-dependent fractional plasticity model can well capture the stress-strain behaviour of different granular soils subjected to a variety of loading conditions.

Acknowledgements
The authors would like to thank Prof. Yannis F. Dafalias for his invaluable suggestions and Prof. Wen Chen for his lifelong inspiration.

Funding
The financial support provided by the National Natural Science Foundation of China (Grant Nos. 41630638, 51679068), the National Key Basic Research Program of China ("973" Program) (Grant No. 2015CB057901) and the China Postdoctoral Science Foundation (Grant No. 2017M621607) is appreciated.

Availability of data and materials
All the data in this study were collected from published literatures, which were appropriately cited.

Competing interests
The authors declare that they have no competing interests.

Authors' contributions
The first author formulated the main ideas and equations of the paper, the second author helped to prepare the figures. All the authors read and approved the final manuscript.

Author details
[1]Key Laboratory of Ministry of Education for Geomechanics and Embankment Engineering, College of Civil and Transportation Engineering, Hohai University, Nanjing, China. [2]School of Civil Engineering, Chongqing University, Chongqing, China.

Publisher's Note

Received: 11 November 2018 Accepted: 22 February 2019 Published online: 01 March 2019

References

1. Li, X., Dafalias, Y.: Dilatancy for cohesionless soils. Geotechnique **50**(4), 449–460 (2000). https://doi.org/10.1680/geot.2000.50.4.449
2. Dafalias, Y.F., Taiebat, M.: SANISAND-Z: zero elastic range sand plasticity model. Geotechnique **66**(12), 999–1013 (2016). https://doi.org/10.1680/jgeot.15.P.271
3. Javanmardi, Y., Imam, S.M.R., Pastor, M., Manzanal, D.: A reference state curve to define the state of soils over a wide range of pressures and densities. Geotechnique **68**(2), 95–106 (2018). https://doi.org/10.1680/jgeot.16.P.136
4. Yang, J., Li, X.: State-dependent strength of sands from the perspective of unified modeling. J. Geotech. Geoenviron. Eng. **130**(2), 186–198 (2004). https://doi.org/10.1061/(ASCE)1090-0241(2004)130:2(186)
5. Ishihara, K.: Liquefaction and flow failure during earthquakes. Geotechnique **43**(3), 351–451 (1993). https://doi.org/10.1680/geot.1993.43.3.351
6. Wan, R., Guo, P.: A simple constitutive model for granular soils: modified stress-dilatancy approach. Comput. Geotech. **22**(2), 109–133 (1998). https://doi.org/10.1016/S0266-352X(98)00004-4
7. Desai, C.S.: Mechanics of Materials and Interfaces: The Disturbed State Concept. CRC Press, Boca Raton (2000)
8. Wang, Z., Dafalias, Y., Li, X., Makdisi, F.: State pressure index for modeling sand behavior. J. Geotech. Geoenviron. Eng. **128**(6), 511–519 (2002). https://doi.org/10.1061/(ASCE)1090-0241(2002)128:6(511)
9. Been, K., Jefferies, M.G.: A state parameter for sands. Geotechnique **35**(2), 99–112 (1985). https://doi.org/10.1016/0148-9062(85)90263-3
10. Schofield, A., Wroth, P.: Critical State Soil Mechanics. McGraw-Hill, London (1968)
11. Rowe, P.W.: The stress-dilatancy relation for static equilibrium of an assembly of particles in contact. Proc. R. Soc. Lond., Ser. A, Math. Phys. Eng. Sci. **269**(1339), 500–527 (1962). https://doi.org/10.1098/rspa.1962.0193
12. Xiao, Y., Liu, H., Chen, Y., Jiang, J.: Bounding surface model for rockfill materials dependent on density and pressure under triaxial stress conditions. J. Eng. Mech. **140**(4), 04014002 (2014). https://doi.org/10.1061/(ASCE)EM.1943-7889.0000702
13. Mortara, G.: A constitutive framework for the elastoplastic modelling of geomaterials. Int. J. Solids Struct. **63**, 139–152 (2015). https://doi.org/10.1016/j.ijsolstr.2015.02.047
14. Sun, Y., Xiao, Y.: Fractional order plasticity model for granular soils subjected to monotonic triaxial compression. Int. J. Solids Struct. **118–119**, 224–234 (2017). https://doi.org/10.1016/j.ijsolstr.2017.03.005
15. Najma, A., Latifi, M.: Predicting flow liquefaction, a constitutive model approach. Acta Geotech. **12**(4), 793–808 (2017). https://doi.org/10.1007/s11440-016-0517-x
16. Tasiopoulou, P., Gerolymos, N.: Constitutive modelling of sand: a progressive calibration procedure accounting for intrinsic and stress-induced anisotropy. Geotechnique **66**(9), 754–770 (2016). https://doi.org/10.1680/jgeot.15.P.284
17. Yang, X.: New rheological problems involving general fractional derivatives with nonsingular power-law kernels. Proc. Rom. Acad., Ser. A: Math. Phys. Tech. Sci. Inf. Sci. **19**(1), 45–52 (2018)
18. Saad, K.M., Baleanu, D., Atangana, A.: New fractional derivatives applied to the Korteweg–de Vries and Korteweg–de Vries–Burger's equations. Comput. Appl. Math. **37**(4), 5203–5216 (2018)
19. Saad, K.M., Atangana, A., Baleanu, D.: New fractional derivatives with non-singular kernel applied to the Burgers equation. Chaos **28**(6), 063109 (2018). https://doi.org/10.1063/1.5026284
20. Saad, K., Al-Sharif, E.H.: Analytical study for time and time-space fractional Burgers' equation. Adv. Differ. Equ. **2017**(1), 300 (2017). https://doi.org/10.1186/s13662-017-1358-0
21. Sun, Y., Shen, Y.: Constitutive model of granular soils using fractional order plastic flow rule. Int. J. Geomech. **17**(8), 04017025 (2017). https://doi.org/10.1061/(ASCE)GM.1943-5622.0000904
22. Sumelka, W., Nowak, M.: Non-normality and induced plastic anisotropy under fractional plastic flow rule: a numerical study. Int. J. Numer. Anal. Methods Geomech. **40**(5), 651–675 (2016). https://doi.org/10.1002/nag.2421
23. Sumelka, W., Nowak, M.: On a general numerical scheme for the fractional plastic flow rule. Mech. Mater. **116**, 120–129 (2018). https://doi.org/10.1016/j.mechmat.2017.02.005
24. Heidarzadeh, H., Oliaei, M.: Development of a generalized model using a new plastic modulus based on bounding surface plasticity. Acta Geotech. **13**(4), 925–941 (2018). https://doi.org/10.1007/s11440-017-0599-0
25. Wheeler, S.J., Näätänen, A., Karstunen, M., Lojander, M.: An anisotropic elastoplastic model for soft clays. Can. Geotech. J. **40**(2), 403–418 (2003). https://doi.org/10.1139/t02-119
26. Pastor, M., Zienkiewicz, O.C., Chan, A.H.C.: Generalized plasticity and the modelling of soil behaviour. Int. J. Numer. Anal. Methods Geomech. **14**(3), 151–190 (1990). https://doi.org/10.1002/nag.1610140302
27. Sun, Y., Gao, Y., Zhu, Q.: Fractional order plasticity modelling of state-dependent behaviour of granular soils without using plastic potential. Int. J. Plast. **102**, 53–69 (2018). https://doi.org/10.1016/j.ijplas.2017.12.001
28. Yang, X., Srivastava, H.M., Machado, J.A.T.: A new fractional derivative without singular kernel: application to the modelling of the steady heat flow. Therm. Sci. **20**(2), 753–756 (2016)
29. Yang, X., Gao, F., Machado, J.A.T., Baleanu, D.: A new fractional derivative involving the normalized sinc function without singular kernel. Eur. Phys. J. Spec. Top. **226**, 3567–3575 (2017)
30. Sun, Y., Gao, Y., Chen, C.: Critical-state fractional model and its numerical scheme for isotropic granular soil considering state-dependence. Int. J. Geomech. **13**(9), 04018202 (2018). https://doi.org/10.1061/(ASCE)GM.1943-5622.0001353

31. Yang, X.-J., Gao, F., Ju, Y., Zhou, H.-W.: Fundamental solutions of the general fractional-order diffusion equations. Math. Methods Appl. Sci. **41**(18), 9312–9320 (2018). https://doi.org/10.1002/mma.5341
32. Sumelka, W.: Fractional viscoplasticity. Mech. Res. Commun. **56**, 31–36 (2014). https://doi.org/10.1016/j.mechrescom.2013.11.005
33. Caputo, M.: Linear models of dissipation whose Q is almost frequency independent-II. Geophys. J. Int. **13**(5), 529–539 (1967). https://doi.org/10.1111/j.1365-246X.1967.tb02303.x
34. Podlubny, I.: Fractional Differential Equations: An Introduction to Fractional Derivatives, Fractional Differential Equations, to Methods of Their Solution and Some of Their Applications. Mathematics in Science and Engineering, vol. 198. Academic Press, San Diego (1998)
35. Caputo, M., Fabrizio, M.: A new definition of fractional derivative without singular kernel. Prog. Fract. Differ. Appl. **1**, 73–85 (2015). https://doi.org/10.12785/pfda/010201
36. Sun, Y., Gao, Y., Shen, Y.: Mathematical aspect of the state-dependent stress-dilatancy of granular soil under triaxial loading. Geotechnique **69**(2), 158–165 (2018). https://doi.org/10.1680/jgeot.17.t.029
37. Sheng, D., Sloan, S.W., Yu, H.S.: Aspects of finite element implementation of critical state models. Comput. Mech. **26**(2), 185–196 (2000). https://doi.org/10.1007/s004660000166
38. Kan, M.E., Taiebat, H.A.: Application of advanced bounding surface plasticity model in static and seismic analyses of Zipingpu Dam. Can. Geotech. J. **53**(3), 455–471 (2015). https://doi.org/10.1139/cgj-2015-0120
39. Bardet, J.P.: Bounding surface plasticity model for sands. J. Eng. Mech. **112**(11), 1198–1217 (1986). https://doi.org/10.1061/(ASCE)0733-9399(1986)112:11(1198)
40. Yu, H., Khong, C., Wang, J.: A unified plasticity model for cyclic behaviour of clay and sand. Mech. Res. Commun. **34**(2), 97–114 (2007). https://doi.org/10.1016/j.mechrescom.2006.06.010
41. Yin, Z.Y., Chang, C.S., Hicher, P.Y., Karstunen, M.: Micromechanical analysis of kinematic hardening in natural clay. Int. J. Plast. **25**(8), 1413–1435 (2009). https://doi.org/10.1016/j.ijplas.2008.11.009
42. Yin, Z.-Y., Chang, C.S., Hicher, P.-Y.: Micromechanical modelling for effect of inherent anisotropy on cyclic behaviour of sand. Int. J. Solids Struct. **47**(14–15), 1933–1951 (2010). https://doi.org/10.1016/j.ijsolstr.2010.03.028
43. Dafalias, Y.F.: Must critical state theory be revisited to include fabric effects? Acta Geotech. **11**(3), 479–491 (2016). https://doi.org/10.1007/s11440-016-0441-0
44. Leoni, M., Karstunen, M., Vermeer, P.A.: Anisotropic creep model for soft soils. Geotechnique **58**(3), 215–226 (2008). https://doi.org/10.1680/geot.2008.58.3.215
45. Seidalinov, G., Taiebat, M.: Bounding surface SANICLAY plasticity model for cyclic clay behavior. Int. J. Numer. Anal. Methods Geomech. **38**(7), 702–724 (2014). https://doi.org/10.1002/nag.2229
46. Xiao, Y., Liu, H., Chen, Y., Jiang, J.: Bounding surface plasticity model incorporating the state pressure index for rockfill materials. J. Eng. Mech. **140**(11), 04014087 (2014). https://doi.org/10.1061/(ASCE)EM.1943-7889.0000802
47. Chen, Q., Indraratna, B., Carter, J., Rujikiatkamjorn, C.: A theoretical and experimental study on the behaviour of lignosulfonate-treated sandy silt. Comput. Geotech. **61**, 316–327 (2014). https://doi.org/10.1016/j.compgeo.2014.06.010
48. Dafalias, Y.F.: Bounding surface plasticity. I: mathematical foundation and hypoplasticity. J. Eng. Mech. **112**(9), 966–987 (1986). https://doi.org/10.1061/(ASCE)0733-9399(1986)112:9(966)
49. Sun, Y., Indraratna, B., Carter, J.P., Marchant, T., Nimbalkar, S.: Application of fractional calculus in modelling ballast deformation under cyclic loading. Comput. Geotech. **82**, 16–30 (2017). https://doi.org/10.1016/j.compgeo.2016.09.010
50. Sasitharan, S., Robertson, P.K., Sego, D.C., Morgenstern, N.R.: State-boundary surface for very loose sand and its practical implications. Can. Geotech. J. **31**(3), 321–334 (1994). https://doi.org/10.1139/t94-040
51. Lee, K.L., Seed, H.B.: Drained strength characteristics of sands. J. Soil Mech. Found. Div. **93**(6), 117–141 (1967)